Precise lattice location of substitutional and interstitial Mg in AlN

L.M. Amorim,[1] U. Wahl,[2] L.M.C. Pereira,[1] S. Decoster,[1] D.J. da Silva,[3] M.R. Silva,[4] A. Gottberg,[5] J.G. Correia,[2] K. Temst,[1] and A. Vantomme[1]

[1)] *Instituut voor Kern-en Stralingsfysica, KU Leuven, 3001 Leuven, Belgium*
[2)] *Centro de Ciências e Tecnologias Nucleares, Instituto Superior Técnico, Universidade de Lisboa, 2686-953 Sacavém, Portugal*
[3)] *IFIMUP and IN-Institute of Nanoscience and Nanotechnology, Universidade do Porto, 4169-007 Porto, Portugal*
[4)] *Centro de Física Nuclear, Universidade de Lisboa, 1649-003, Portugal*
[5)] *CERN-ISOLDE, 1211 Geneva 23, Switzerland*

(Dated: 29 November 2013)

The lattice site location of radioactive ^{27}Mg implanted in AlN was determined by means of emission channeling. The majority of the ^{27}Mg was found to substitute for Al, yet significant fractions (up to 33%) were also identified close to the octahedral interstitial site. The activation energy for interstitial Mg diffusion is estimated to be between 1.1 eV and 1.7 eV. Substitutional Mg is shown to occupy ideal Al sites within a 0.1 Å experimental uncertainty. We discuss the absence of significant displacements from ideal Al sites in the context of the current debate on Mg doped nitride semiconductors.

PACS numbers: 61.85.+p, 61.72.Cc, 68.55.Ln, 61.72.uj

CERN-OPEN-2014-013
04/11/2013

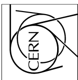

The group-III nitride semiconductors are of special interest, not only from a fundamental point of view, but particularly in the context of applications. This is largely due to the ability to obtain semiconductors with a direct band-gap ranging from 0.675 eV[1] to 6.12 eV,[2] by alloying GaN with either InN or AlN. AlN in particular, having the widest direct band gap, exhibits excellent optical and dielectric properties, thermal conductivity and mechanical hardness, with applications in deep ultra-violet light emitting diodes (down to 210 nm[3,4]), ultra-violet detectors, laser diodes, surface acoustic wave devices (SAWs), high temperature electronics and pressure converters.[5] While unintentionally doped nitrides typically show n-type behavior, p-type doping of GaN is routinely achieved by the introduction of the group II element Mg, which replaces the group III cation Ga (forming $\mathrm{Mg_{Ga}}$). Efficient p-type doping is only obtained after proper electrical activation procedures, since $\mathrm{Mg_{Ga}}$ acceptors tend to be passivated by H impurities. Thermal treatment above 500 °C is considered to out-diffuse the H impurities and activate the Mg acceptors in GaN.[6] Finding a suitable acceptor for the extreme wide gap compound AlN is, however, far more challenging. Theoretical predictions regarding the best choice of acceptor for AlN differ considerably: while many favor Be on Al sites ($\mathrm{Be_{Al}}$)[5,7–9] others have argued that $\mathrm{Mg_{Al}}$ should be the most suitable acceptor.[10–12] So far, acceptor behavior has been claimed experimentally for $\mathrm{Mg_{Al}}$ with an ionization energy around 500-630 meV,[4,13,14] as well as for $\mathrm{Be_{Al}}$ with ∼330 meV.[15]

In most theoretical work, only substitutional $\mathrm{Mg_{Al}}$ on ideal Al sites has been considered, since interstitial Mg, which acts as donor,[16] was suggested to be unstable.[10] Based on *ab initio* calculations for substitutional $\mathrm{Mg_{Al}}$ in AlN, Lyons *et al.*[17] have recently proposed that in the ionized state ($\mathrm{Mg_{Al}^-}$) Mg occupies a *near-ideal* Al site, whereas in the neutral state ($\mathrm{Mg_{Al}^0}$) the Mg atom is displaced from the ideal substitutional Al site. The shift results from the localization of the Mg-related hole on a N neighbor along the c-axis, which leads to an increase in the Mg-N bond length by 18% (0.34 Å), accommodated by displacements of both the Mg atom and its N neighbor (along the c-axis). On the other hand, the ab initio calculations of Szabó *et al.*[12] suggest for the acceptor state elongations of the Mg-N bond lengths by ∼0.2 Å along the c-axis and ∼0.13 Å basal to it, which should result in only small displacements of Mg from the ideal Ga site. These inconsistencies, which in fact also exist for Mg in GaN,[17–19] can only be clarified by a precise experimental determination of the Mg lattice location.

In this letter, we report on direct lattice location studies of implanted Mg in AlN. Using the β^- emission channeling technique,[20–23] we are able to precisely probe the lattice sites occupied by radioactive impurities in single crystalline samples. Following the decay of the radioactive probes, the emitted β^- particles experience *channeling* and *blocking* effects imposed by the periodic arrangement of the positive nuclei of the single crystal. β^- particles (electrons) that are emitted within a critical angle around high symmetry directions of the crystal are *channeled* while those emitted at higher angles are randomly scattered (*blocked*). The resulting angle-dependent emission yield, characteristic of the lattice site occupied by the probe atom, is measured in the vicinity of low-index axes of the single crystal using a 2-dimensional position-sensitive detector. Typically, four different axes are chosen which allow for the unambiguous distinction of the different lattice sites.

The production of radioactive Mg beams at CERN's on-line isotope separator facility ISOLDE by means of bombarding a $\mathrm{UC_2}$ target with 1.4 GeV protons, followed by laser ionization, is described in Ref. 24. The only radioactive isotope of Mg suitable for emission channeling studies is the short-lived ^{27}Mg ($t_{1/2}$ =9.45 min). Due to

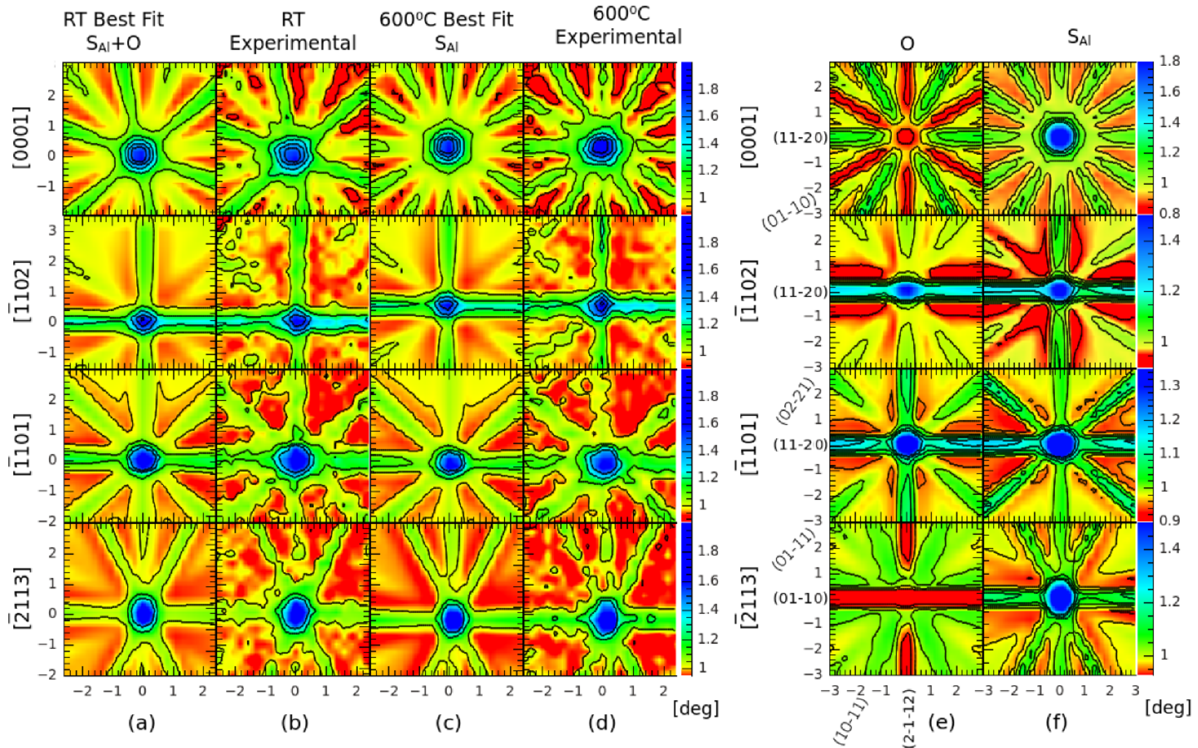

FIG. 1. (a)-(d) Comparison of the experimental emission channeling patterns around [0001], [$\bar{1}$102], [$\bar{1}$101] and [$\bar{2}$113] directions of sample B for room temperature (RT, (b)) and 600 °C (d) implantation with the best fit simulated patterns. (e)-(f) The theoretical patterns for 100% of ^{27}Mg on O (e) and S_{Al} (f) sites, respectively. While the temperature used for the simulated patterns in (e)-(f) was in both cases RT, the fits for 600 °C measurements (c) used patterns calculated for that temperature (not shown).

the short half-life of ^{27}Mg, emission channeling measurements must be performed either during ^{27}Mg implantation into the sample, or during its decay within about 30 min after implantation. The experimental on-line setup used for that purpose is described in Ref. 25.

Three different AlN samples were measured. Samples A and B consist of 3 μm thin films grown by hydride vapor phase epitaxy (HVPE) on sapphire. Sample C is a 1 μm thin film grown by physical vapor deposition process. Sample A was only implanted and measured at room temperature (RT) with a total ^{27}Mg fluence of about 1.5×10^{12} cm^{-2}. Samples B (5×10^{12} cm^{-2}) and C (9×10^{12} cm^{-2}) were implanted and measured at higher temperatures, with each temperature step requiring around 50 min of measuring time. All samples were implanted using an energy of 50 keV. After these low-fluence measurements, sample C was implanted with 1×10^{15} cm^{-2} of stable ^{24}Mg, and the ^{27}Mg emission channeling measurements were then repeated for annealing temperatures up to 600 °C. For this high-fluence experiment, the Mg peak concentration is estimated to be $\sim1.5\times10^{20}$ cm^{-3}, i.e. within the concentration regime reported for the electrical doping of AlN.[4,14]

Quantitative information is obtained by fitting the experimental emission yields with theoretical patterns for the various possible lattice sites, calculated using the *manybeam* formalism for electron channeling.[20,22] Experimental and theoretical data on the crystallographic structure of AlN and the RT root mean square (rms) displacements of Al and N atoms can be found in Refs. 26–28. The rms displacements (u_1) of Al and N atoms at room temperature were assumed to be isotropic with $u_1(Al)$=0.0569 Å and $u_1(N)$=0.0626 Å, based on Ref. 27. Since $u_1(Al)$ and $u_1(N)$ are unknown at higher temperatures, these parameters were extrapolated from their RT values assuming a Debye model and Debye temperatures of $T_D(Al)$=765 K and $T_D(N)$=878 K (estimated from the u_1 values at RT[29]). Manybeam calculations were performed for a number of discrete electron energies which were then averaged according to the continuous β^- spectrum of ^{27}Mg (average β energy 703 keV, endpoint energy 1767 keV) as described in Ref. 30. Some of the sites which were considered as possible impurity positions in GaN have been previously described[31] and the whole set is shown in a figure included in the supplemental material to this article.[32] The fit procedure is described in Refs. 22 and 23. The columnar mosaic domains of the AlN thin films were accounted for as described in Ref. 33 (lattice mosaic spreads of $W_{tilt}\sim0.2°$ and $W_{twist}\sim0.62°$ were determined using the method of Srikant[34]).

Figure 1(d) shows the experimental emission channeling patterns measured from sample B during 600 °C im-

plantation. Simple visual comparison to the expected patterns for 100% of ^{27}Mg atoms on substitutional Al sites S_{Al} [Fig.1(f)] suggests that the majority of the ^{27}Mg occupies S_{Al} sites. This is confirmed by the quantitative fit: the best fit shown in Fig.1(c) corresponds to 97% of ^{27}Mg on S_{Al} sites, with only 3% remaining on *random* sites. The experimental patterns obtained from the same sample for RT implantation are shown in Fig.1(b). While the overall channeling effects are quite similar to those corresponding to 600 °C implantation, there are distinct differences which suggest the occupancy of an additional lattice site. Most prominently, the channeling effects along the set of $(01\bar{1}0)$ planes in the [0001] and $[\bar{2}113]$ patterns are considerably reduced, while the set of $(11\bar{2}0)$ planes and also the $[\bar{1}102]$ and $[\bar{1}101]$ axes still exhibit prominent channeling effects. These features are characteristic of interstitial sites near the octahedral O position. This is fully confirmed by the best fit [Fig.1(a)], which is obtained for a linear combination of 73±5% on S_{Al} and 25±4% located near the O interstitial sites. Allowing for O occupancy results in an improvement of up to 20% in χ^2 for the [0001] patterns.

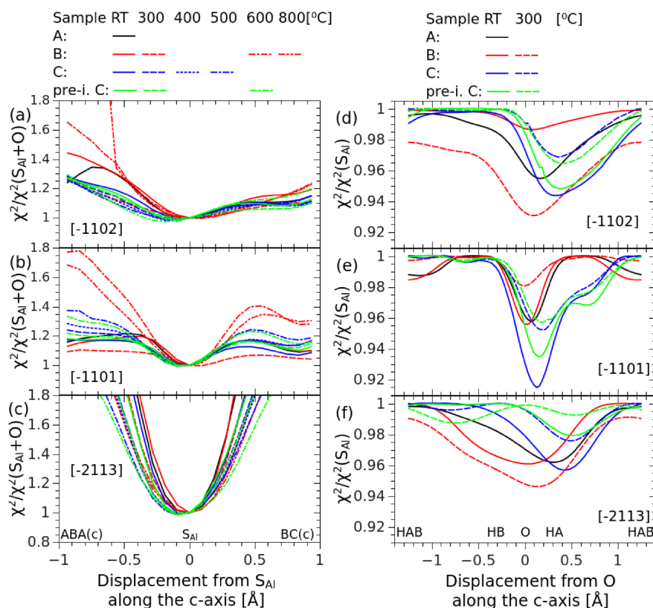

FIG. 2. (a)-(c) Reduced χ^2 of the fits to the experimental $[\bar{1}102]$, $[\bar{1}101]$, and $[\bar{2}113]$ patterns as function of displacement of the ^{27}Mg atoms from the ideal substitutional S_{Al} sites along the c-axis. Each data point corresponds to the χ^2 of the best fit obtained using two given sites, with the corresponding two fractions as free parameters. The site pairs are composed of a fixed interstitial site near the octahedral O position, plus a second site which is shifted from the ideal substitutional S_{Al} site along the c-axis. The reduced χ^2 was normalized to the minimum value of each curve. (d)-(f) Reduced χ^2 as function of displacement of the ^{27}Mg atoms from the ideal interstitial O sites along the c-axis. The site pairs are composed of a fixed S_{Al} site plus a second site which is shifted from the ideal interstitial O site along the c-axis. The reduced χ^2 was, in this case, normalized to that of the one-site S_{Al} fit.

We have also investigated eventual displacements of substitutional and interstitial ^{27}Mg from the ideal S_{Al} and O sites, respectively. Figure 2 shows the fit χ^2 as a function of the displacement along the c-axis. Similar results were found for displacements along the basal bond directions, and if the two site-displacements (for the substitutional and the interstitial fractions) are allowed to vary simultaneously. The χ^2 [Fig.2(a)-(c)] displays clear minima for displacements from the ideal S_{Al} sites of at most 0.1 Å. At first sight, if one assumes that all the substitutional Mg dopants in our samples are in the neutral state, our results seem to support the prediction of Szabó *et al.*[12] and contradict that of Lyons *et al.*[17]: if an elongation of Mg-N c-axis bond length does occur, it must be accommodated by a displacement of the N neighbor, without significantly displacing the Mg atom from the ideal Al site. On the other hand, if all substitutional Mg acceptors in our samples are in the ionized state (compensated by native donor defects, possibly created upon ^{27}Mg implantation), our results are perfectly consistent with the prediction of Lyons *et al.*[17], i.e. that ionized Mg acceptors are not associated with significant displacements. In reality, it is much more likely that, at least for some combination of Mg concentration and implantation temperature in our samples, we have a mixture of neutral and ionized Mg acceptors. Since we observe no displacement (within 0.1 Å) from the ideal S_{Al} site, regardless of Mg concentration and implantation temperature, our data suggest that substitutional Mg in AlN is not significantly displaced in either neutral or ionized states. For the displacements from the O interstitial sites, the picture is somewhat less clear [Fig.2(d)-(f)] since the maximum interstitial fraction is only ∼33% and the channeling and blocking patterns of the interstitial sites exhibit less anisotropy than in the case of substitutional S_{Al} sites. Consequently, the experimental patterns are far less influenced by changes in the positions of the interstitial emitter atoms. Nevertheless the observed minima are located within a region that stretches roughly ∼0.5 Å from the ideal O site towards HA (hexagonal near Al atoms) site. In particular, all the χ^2 minima for the $[\bar{1}101]$ direction, which appears to be more sensitive for such displacements, are located within ∼0.2 Å from the ideal O towards the HA site. We therefore conclude that the displacement from the ideal O sites is, at most, 0.5 Å, most likely $\lesssim$0.2 Å.

Figure 3 shows the fitted fractions of ^{27}Mg on S_{Al} and near-O sites as a function of implantation and measurement temperature for all samples. The error bars are the standard deviation obtained when averaging the fitted fractions for the four different directions of each sample. For RT implantation, 20–33% of the ^{27}Mg was found on near-octahedral interstitial O sites and 63–70% on substitutional Al sites. For implantation temperatures around 300−400 °C the near-O interstitial Mg is partially converted to S_{Al} sites, a process which is completed at 500 °C. Up to the highest implantation temperature of 800 °C only S_{Al} sites are found. For sample C, in comparison

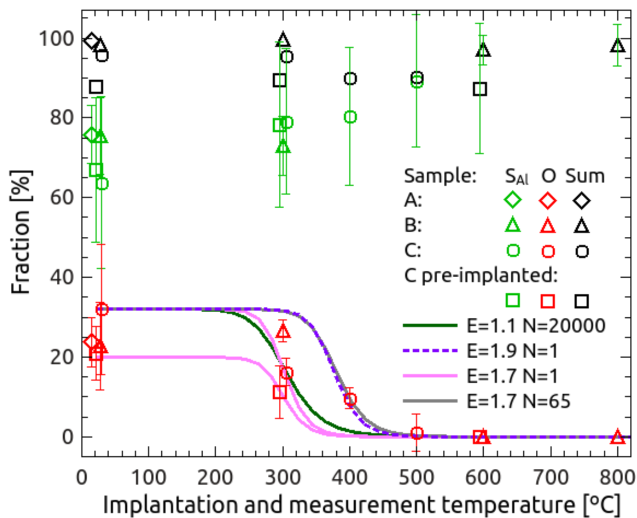

FIG. 3. The substitutional S_{Al} and near-octahedral O fractions of ^{27}Mg as a function of the implantation and measurement temperature for all samples. The sum of the two fractions, which in the absence of a random fraction should amount to 100%, is also shown. The solid lines correspond to the near-O fractions expected for the Arrhenius models for migration and capture of interstitial Mg in sample C (cf. discussion in the text) with different energies E_M and steps N.

to the ^{27}Mg low-fluence (9×10^{12} cm^{-2}) results, the pre-implantation of 1×10^{15} cm^{-2} of ^{24}Mg leads to some increase of the substitutional and random ^{27}Mg fractions at the expense of interstitial ^{27}Mg, but the overall behavior is very similar.

The fact that the near-O interstitial ^{27}Mg is converted to S_{Al} sites in a relatively narrow temperature regime can be used to estimate the activation energy required for this process. For that purpose, we assume that interstitial Mg starts to migrate and diffuse until it encounters an Al vacancy by which it is trapped and thus converted to substitutional. This is a common trapping mechanism of diffusing interstitial impurities in semiconductors (quantitative models have been described in Ref. 29 for implanted ^{8}Li). In thermal equilibrium the fraction of interstitial Mg $f_i(T)$ at a given temperature T is given by

$$\frac{f_i(T)}{f_{i0}} = \frac{1}{1 + e^{-\frac{E_M}{k_B T}} \nu_0 \frac{\tau}{N}}, \quad (1)$$

where f_{i0} is the fraction of interstitial Mg present in the sample directly following implantation (assumed to be the same fractions as at RT), τ is the radioactive lifetime of ^{27}Mg, E_M is the activation energy for migration of interstitial Mg and ν_0 its attempt frequency, and N the number of jumps before an interstitial Mg reaches an Al vacancy. Limits for the number of steps can be obtained by considering two extreme cases: N=1 if interstitial Mg and an Al-vacancy are located on nearest-neighbor sites; $N\sim$200000 if the diffusion length is comparable to the implantation depth. Similar estimates are described in more detail in Ref. 35. The magenta and green curves in Fig.3 correspond to the two extreme cases for the site change in sample C. The case with $N\sim$200000 (green curve) provides a lower limit for the activation energy of E_M=1.1 eV, whereas the 1-step model gives E_M=1.7 eV (two magenta curves, for the low-fluence and high-fluence case, respectively). The exact value of E_M is likely to be closer to 1.7 eV, since one can expect a significant concentration of Al vacancies resulting from the ^{27}Mg implantation. The other two curves in Fig.3 illustrate how the different parameters of the model (either E_M or N) influence in the expected interstitial fraction.

In conclusion, we have determined the lattice location of the implanted p-type dopant ^{27}Mg in AlN. For room temperature implantation, the majority (63–70%) of ^{27}Mg was found in substitutional Al sites, while a significant fraction of 20–33% was also identified close to the octahedral interstitial O site of AlN. For implantation at 600 °C and above, the octahedral interstitial fraction is converted to Mg on S_{Al} sites, which is attributed to the migration of interstitial Mg that is thermally activated around 300–400 °C with an activation energy estimated between 1.1 and 1.7 eV. It is likely that we were able to observe significant fractions of interstitial Mg thanks to the particular incorporation dynamics of ion implantation. The far-from-equilibrium nature of the implantation process promotes the occupation of lattice sites with high formation energies, which are therefore not observed when the dopants are incorporated under typical growth conditions. In any case, our results show that interstitial Mg will in general not be observed, since its thermal stability is far below the typical growth temperature of AlN thin films. Regarding substitutional Mg, a detailed study of possible displacements from ideal Al sites revealed that those must be smaller than 0.1 Å, which establishes strong limits for proposed models of the local structure of Mg dopants in AlN. In general, our findings illustrate how precise and unambiguous lattice location techniques are crucial for the understanding of intricate doping mechanisms.

This work was funded by the Portuguese Foundation for Science and Technology (CERN/FP/123585/2011), the European Commission through the SPIRIT (Support of Public and Industrial Research using Ion beam Technology, Contract 227012), the ENSAR (European Nuclear Science and Applications Research, Contract 262010) projects, the FWO (the Fund for Scientific Research Flanders) and the KU Leuven research fund (Project No. GOA/09/006 and GOA/14/007). The authors further acknowledge the ISOLDE collaboration for supportive access to beam time.

[1] P. Schley, R. Goldhahn, G. Gobsch, M. Feneberg, K. Thonke, X. Wang, and A. Yoshikawa, Phys. Status Solidi B **246**, 1177 (2009).

[2] J. Li, K. Nam, M. Nakarmi, J. Lin, H. Jiang, P. Carrier, and S. Wei, Appl. Phys. Lett. **83**, 5163 (2003).

[3] A. Khann, A. Balakrishnan, and T. Katona, Nature Photonics **2**, 77 (2008).
[4] Y. Taniyasu, M. Kasu, and T. Makimoto, Nature **441**, 325 (2006).
[5] F. Mireles and S. Ulloa, Phys. Rev. B **58**, 3879 (1998).
[6] S. Nakamura, N. Iwasa, M. Senoh, and T. Mukai, Jpn. J. Appl. Phys. **31**, 1258 (1992).
[7] A. Fara, F. Bernardini, and V. Fiorentini, J. Appl. Phys. **85**, 2001 (1999).
[8] R. Wu, L. Shen, M. Yang, Z. Sha, Y. Cai, Y. Feng, Z. Huang, and Q. Wu, Appl. Phys. Lett. **91**, 152110 (2007).
[9] Y. Zhang, W. Liu, and H. Niu, Phys. Rev. B **77** (2008).
[10] C. V. de Walle and J. Neugebauer, J. Appl. Phys. **95**, 3851 (2004).
[11] C. Stampfl and C. V. de Walle, Phys. Rev. B **65**, 1 (2002).
[12] A. Szabó, N. Son, E. Janzén, and A. Gali, Appl. Phys. Lett. **96**, 192110 (2010).
[13] K. Nam, M. Nakarmi, J. Li, J. Lin, and H. Jiang, Appl. Phys. Lett. **83**, 878 (2003).
[14] M. Nakarmi, N. Nepal, C. Ugolini, T. Altahtamouni, J. Lin, and H. Jiang, Appl. Phys. Lett. **89**, 152120 (2006).
[15] A. Sedhain, T. A. Tahtamouni, J. Li, J. Lin, and H. Jiang, Appl. Phys. Lett. **93**, 141104 (2008).
[16] J. Neugebauer and C. V. de Walle, J. Appl. Phys. **85**, 3003 (1999).
[17] J. Lyons, A. Janotti, and C. V. de Walle, Phys. Rev. Lett. **108**, 155212 (2012).
[18] S. Lany and A. Zunger, Appl. Phys. Lett. **96**, 142114 (2010).
[19] J. J. Davies, Phys. Rev. B **87**, 235208 (2013).
[20] H. Hofsäss and G. Lindner, Physics Reports **201**, 121 (1991).
[21] U. Wahl, J. Correia, S. Cardoso, J. Marques, A. Vantomme, and G. Langouche, Nucl. Instrum. Methods B **136**, 744 (1998).
[22] U. Wahl, Hyperfine Interactions **129**, 349 (2000).
[23] U. Wahl, J. G. Correia, A. Czermak, S. Jahn, P. Jalocha, J. Marques, A. Rudge, F. Schopper, J. C. Soares, and A. Vantomme, Nuc. Inst. Meth. A **524**, 245 (2004).
[24] U. Köster, V. N. Fedoseyev, A. N. Andreyev, U. C. Bergmann, R. Catherall, J. Cederkäll, M. Dietrich, H. D. Witte, D. V. Fedorov, L. Fraile, S. Franchoo, H. Fynbo, U. Georg, T. Giles, M. Gorska, M. Hannawald, M. Huyse, A. Joinet, O. C. Jonsson, K. L. Kratz, K. Kruglov, C. Lau, J. Lettry, V. I. Mishin, M. Oinonen, K. Partes, K. Peräjärvi, B. Pfeiffer, H. L. Ravn, M. D. Seliverstov, P. Thirolf, K. V. de Vel, P. V. Duppen, J. V. Roosbroeck, L. Weissman, IS365, IS387, IS393, and I. Collaborations, Nucl. Inst. Meth. B **204**, 347 (2003).
[25] M. R. Silva, U. Wahl, J. G. Correia, L. M. Amorim, and L. M. C. Pereira, Rev. Sci. Instrum. **1**, 1 (2013).
[26] H. Schulz and K. H. Thiemann, Sol. State Comm. **23**, 815 (1977).
[27] E. Gabe and Y. Page, Phys. Rev. B **24**, 5634 (1981).
[28] M. Schowalter, A. Rosenauer, J. T. Titantah, and D. Lamoen, Acta Crys. A **65**, 227 (2009).
[29] U. Wahl, Physics Reports **280**, 145 (1997).
[30] U. Wahl, J. G. Correia, T. Mendonca, and S. Decoster, Appl. Phys. Lett. **94**, 261901 (2009).
[31] U. Wahl, J. Correia, E. Rita, E. Alves, J. Soares, B. D. Vries, V. Matias, A. Vantomme, and the ISOLDE collaboration, Hyperfine Interactions **159**, 363 (2005).
[32] See supplemental material at [URL will be inserted by AIP] for a description of the experimental details and of the interstitial sites.
[33] B. Vries, U. Wahl, J. Correia, S. Ruffenach, O. Briot, and A. Vantomme, Appl. Phys. Lett. **103**, 172108 (2013).
[34] V. Srikant, J. Speck, and D. Clarke, J. Appl. Phys. **82**, 4286 (1997).
[35] L. Pereira, U. Wahl, S. Decoster, J. Correia, M. da Silva, and A. Vantomme, Appl. Phys. Lett. **98**, 201905 (2011).